Heliyon 10 (2024) e31242

Contents lists available at ScienceDirect

Heliyon

journal homepage: www.cell.com/heliyon

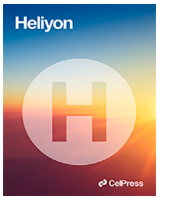

Research article

A fractional order model for the transmission dynamics of shigellosis

Stephen Edward

Department of Mathematics and Statistics, University of Dodoma, Postal address: Box 338, Dodoma, Tanzania

ARTICLE INFO

Keywords:
Memory
Predictor-corrector method
Caputo fractional derivative
Control strategies
Ulam-Hyers stability

ABSTRACT

Shigellosis, a highly contagious bacterial infection causing diarrhea, fever, and abdominal pain, necessitates a deep understanding of its transmission dynamics to devise effective control measures. Our study takes a novel approach, employing a fractional order framework to explore the influence of memory and control measures on *Shigellosis* transmission dynamics, thereby making a unique contribution to the field. The model is presented as a system of Caputo fractional differential equations capturing time constant controls. The Caputo derivatives are chosen for their inherent benefits. The qualitative features of the model, such as the solutions' existence and uniqueness, positivity, and boundedness, are thoroughly investigated. Moreover, the equilibria of the model are derived and analyzed for their stability using suitable theorems. In particular, local stability was proved through Routh's criteria, while global stability results were established in the Ulam-Hyers sense. The model is then solved numerically with the help of the predict-evaluate-correct-evaluate method of Adams-Bashforth-Moulton. The numerical results underscore the significant impact of memory on disease evolution, highlighting the novelty of integrating memory-related aspects into the meticulous planning of effective disease control strategies. Using fractional-order derivatives is more beneficial for understanding the dynamics of *Shigellosis* transmission than integral-order models. The advantage of fractional derivatives is their ability to provide numerous degrees of freedom, allowing for a broader range of analysis of the system's dynamic behaviour, including nonlocal solutions. Also, an investigation on the impacts of control measures via parameter variation is done; the findings show that applying treatment and sanitation minimizes disease eruption.

1. Introduction

Shigellosis, often known as bacterial dysentery, has a remarkably high incidence in children under five in mid and low-income nations. It is accountable for an estimated 1.1 million fatalities annually on a global scale. Almost 66% of deaths resulting from the disease relate to those that fall under the age of five years or less [1,2]. Furthermore, it is widespread among travellers and men who participate in same-sex relationships (MSM) in countries with higher incomes [3,4]. *Shigellosis* is a gastrointestinal infectious illness attributed to the presence of Shigella bacteria. The bacterial strains under consideration may be classified into four distinct subgroups, specifically S. flexneri, *S. dysenteriae 1*, and *S. boydii* [5]. Extreme outbreaks of dysentery are typically attributed to the presence of S. dysenteriae 1, a strain that generates Shiga toxins. In contrast, the disease's most prevalent and ongoing cases are

E-mail address: stephen.edward@udom.ac.tz.

https://doi.org/10.1016/j.heliyon.2024.e31242
Received 7 May 2024; Accepted 13 May 2024

Available online 16 May 2024

caused mainly by S. flexneri and S. sonnei [6]. *Shigellosis* outbreaks commonly strike places with high population density, especially those with inadequate sanitation facilities. According to the study by [7], the main methods of disease transmission frequently involve direct contact with other people or the contamination of food and water supplies by the Shigella bacteria. In the early 20th century, housing, sanitation, and hygiene improvements considerably reduced the incidence of asylum dysentery in the civilian population. The advent of antibiotics and their application to treating dysentery also contributed to curtailing transmission [8].

The disease is characterized by elevated body temperature, acute stomach spasms, and urgent sensations in the rectal area. The lack of effective therapies contributes to an increased risk of life-threatening symptoms. Unluckily, the absence of an accessible vaccination for the disease persists despite numerous and varied approaches to vaccine development [9,10]. Asymptomatic infected humans present a possible challenge in managing and controlling infectious illnesses, such as *Shigellosis*. The issue commonly occurs since asymptomatic infected humans do not exhibit clinical symptoms, inadvertently perpetuating the spread of infection. Given the absence of symptoms, persons who do not display any signs of the disease are often overlooked in efforts aimed at disease management, including treatments and quarantine or isolation measures. Therefore, it is crucial to investigate the roles of asymptomatic humans in influencing the spread of *Shigellosis* infections.

A thorough investigation of *Shigellosis* has been conducted through various studies employing mathematical models, including noteworthy contributions by researchers such as [11–15]. The work by [11] considered an SIRS (Susceptible-Infectious-Recovered-Susceptible) model where they assumed the main pathway through which *Shigellosis* could be contracted was direct transmission, i.e. human-to-human transmission; they did not consider indirect transmission, such as consuming contaminated food or water. On the other hand, [12] studied *Shigellosis* by a SEAIR-B (Susceptible-Exposed-Asymptomatic-Infectious-Recovered-Bacteria) model that also captured the carrier compartment and dual transmission mechanisms. Also, [13] studied *Shigellosis* via a SIRB model capturing direct and indirect transmission routes. In recent work, *Shigellosis* was investigated by [14] with a focus on dual transmission dynamics and the incorporation of fixed parameters associated with control strategies such as medical treatment, proper sanitation, and health promotion programs. Later, [15] modified the work by [14] to capture time-dependent controls and investigated how they could be used most economically and still reduce the number of infected individuals.

Most studies on *Shigellosis* available in literature such as [11–15] use integer calculus differential equations, which describe a Markovian epidemic process. However, surveys show a non-Markovian transmission process [17,18]. Fractional-order models are increasingly used in scientific and technical fields due to their advantages, such as flexibility, better approximation, improved memory handling, system identification, anomalous behaviour representation, and stability analysis [16]. Fractional derivatives capture many systems' memory and hereditary characteristics, providing an improved modelling approach for examining disease transmission dynamics in conventional settings. Knowledge about past disease incidence and countermeasures can significantly impact the present situation.

Fractional calculus has been used to study problems in mathematical biology and epidemiology, including chaotic behaviour, physics principles, COVID-19 transmission dynamics, Hepatitis C infection, DNA dynamics, cancer modelling, epidemic models, ethanol concentration, and deforestation effects [20–35]. Recent approaches for generalizing fractional-order differentiation are available include the Riemann-Liouville, Caputo-fractional derivative [36,51,52], Caputo–Fabrizio fractional derivative [37,54], and Antagana-Baleanu function approaches [38,53].

While numerous fractional derivatives exist in the literature; the Caputo fractional derivative is one of the most widely used techniques in fractional calculus. By employing such techniques, we can gain deeper insights into the complex behaviours of natural systems, which can help us better understand and predict their behaviour. Utilizing the Caputo fractional derivative offers a significant benefit in maintaining the same initial conditions as traditional derivatives [39].

Compared with previous studies such as [11–15], the main contributions of this work are to extend the findings by [14] to the Caputo fractional order derivative model that will capture treatment, sanitation, and screening control measures and evaluate the role of memory in the transmission dynamics of *shigellosis* infection. Precisely, the main contributions are:

- Development of the Caputo framework for shigellosis transmission dynamics.
- Ulam-Hyers stability for the proposed model has been presented.
- PECE algorithm for numerical solution has been proposed.
- Memory effect has been investigated.

The remaining parts of the article comply with the following organizational setup: Section 2 explores key concepts associated with the fractional operator and Laplace transform. Section 3 presents a fractional mathematical model based on Caputo's sense. Section 4 focuses on analyzing the fractional differential equation (FDE) model built in section 3. Section 5 provides a numerical scheme that employs the predict-evaluate-correct-evaluate (PECE) method of Adams–Bashforth–Moulton (ABM) to solve the FDE developed. Section 6 presents numerical simulations, and Section 7 concludes the article by giving closing remarks.

2. Preliminaries

This section will present some necessary definitions and notations related to fractional calculus. The Riemann-Liouville and Caputo definitions are the most often employed.

Remark 1. A real function f is said to be of class C, if f is piecewise continuous on $[a, b]$ and integrable on any finite subinterval of $[a, b]$.

Definition 1. The left and right Riemann-Liouville fractional (R-LF) integrals $I^{\alpha}_{a+}f$ and $I^{\alpha}_{b-}f$ of order $\alpha \in \mathbb{C}(Re(\alpha)) > 0$ are, respectively, defined by [36]

$$I^{\alpha}_{a+}f(t) = \frac{1}{\Gamma(\alpha)} \int_{a}^{t} (t-s)^{\alpha-1} f(s) ds, \tag{1}$$

and

$$I^{\alpha}_{b-}f(t) = \frac{1}{\Gamma(\alpha)} \int_{t}^{b} (t-s)^{\alpha-1} f(s) ds, \tag{2}$$

where $\Gamma(.)$ is the Euler gamma function.

Definition 2. [36] The left and right Riemann-Liouville fractional derivatives $D^{\alpha}_{a+}f$ and D^{α}_{b-} of order $\alpha \in \mathbb{C}(Re(\alpha)) > 0$ are, respectively, defined by

$$(D^{\alpha}_{a+}f)(t) = (\frac{d}{dt})^{n}(I^{n-\alpha}_{a+}f)(t), \tag{3}$$

and

$$(D^{\alpha}_{b-}f)(t) = (-\frac{d}{dt})^{n}(I^{n-\alpha}_{b-}f)(t), \tag{4}$$

where $n = [Re(\alpha)] + 1$ and $Re(\alpha)$ is the greatest integer less than or equal to $Re(\alpha)$.

Definition 3. [36] The left and right Caputo-fractional derivatives ${}^{C}D^{\alpha}_{a+}f$ and ${}^{C}D^{\alpha}_{b-}f$ of order $\alpha \in \mathbb{C}(Re(\alpha)) > 0$ are, respectively, defined by

$$({}^{C}D^{\alpha}_{a+}f)(t) = (I^{n-\alpha}_{a+}f^{(n)})(t) = \frac{1}{\Gamma(n-\alpha)} \int_{a}^{t} \frac{f^{(n)}(s)}{(t-s)^{\alpha-n+1}} ds, \tag{5}$$

and

$$({}^{C}D^{\alpha}_{b-}f^{(t)})(t) = (-1)^{n}(I^{n-\alpha}_{b-}f^{(n)})(t) = \frac{(-1)^{n}}{\Gamma(n-\alpha)} \int_{t}^{b} \frac{f^{(n)}(s)}{(t-s)^{\alpha-n+1}} ds. \tag{6}$$

Theorem 1. *[41] (Generalized Mean Value Theorem) Suppose that* $f(t) \in C[a,b]$ *and* ${}^{C}_{0}D^{\alpha}_{t}f(t) \in C[a,b]$ *for* $0 < \alpha \leq 1$. *Then, we have*

$$f(t) = f(a) + \frac{1}{\Gamma(\alpha)}({}^{C}_{a}D^{\alpha}_{\epsilon}f(\epsilon))(t-a)^{\alpha},$$

where $a \leq \epsilon \leq t, \forall_{t} \in [a,b]$.

Definition 4. [40] For $\alpha, \beta, z \in \mathbb{C}$ with $Re(\alpha) > 0$, the classical Mittag-Leffler functions are defined by

$$E_{\alpha,\beta}(z) = \sum_{k=0}^{\infty} \frac{z^{k}}{\Gamma(\alpha k + \beta)}, \tag{7}$$

for $\beta = 1$, it is written that

$$E_{\alpha}(z) \triangleq E_{\alpha,1}(z) = \sum_{k=0}^{\infty} \frac{z^{k}}{\Gamma(\alpha k + 1)}. \tag{8}$$

Definition 5. [36] Let $F(s)$ be the Laplace transform of the function $f(t)$. Then, the Laplace transform of the Caputo derivative is given by

$$(\mathcal{L}\,{}^{C}D^{\alpha}_{0+}f(t))(s) = s^{\alpha}(\mathcal{L}f(t))(s) - \sum_{j=0}^{l-1} d_{j} s^{\alpha-j-1}, \tag{9}$$

where $l - 1 < \alpha \leq l, l \in \mathbb{N}$ and with

$$d_{j} = f^{(j)}(0)(j = 0, 1, ..., l-1).$$

Table 1
A complete list of detailed parameters and their corresponding baseline values.

Parameter	Explanation	Value	Source
Λ	The enrollment rate of persons into the vulnerable compartment.	469 Humans/year	[13]
α_1	Transmission rate for symptomatic infectious population.	0.4/year	[13]
α_2	Transmission rates for asymptomatic infectious humans.	0.6/year	[13]
α_3	Rate at which humans ingest contaminated fecal matter.	0.4465/year	[11]
δ	Rate of latency (period for which the latent humans, $E(t)$ start to portray signs of infections).	0.35/day	[12]
μ	Natural human mortality rate.	1/50/year	[44]
d_1	Disease-induced mortality rate for symptomatic infectious humans.	0.02 /year	Assumed
d_2	Disease-induced mortality rate for asymptomatic infectious humans.	0.03 /year	Assumed
η_1	Rate of healing for the symptomatic infectious individuals.	0.14/day	[43]
η_2	Asymptomatic humans' recovery rate.	0.026/day	[12]
ϵ_1	The rate of pathogen discharge into the water supply by persons who are infected and portray symptoms.	80 cells/mL/day	Assumed
ϵ_2	The rate of pathogen discharge into the water supply by infected persons who show no symptoms.	70 cells/mL/day	Assumed
μ_b	Depletion rate for Shigella.	0.83/day	Assumed
ϕ	Loss of temporal disease-induced immunity.	0.25 /year	[43]
χ	Sanitation-induced death rate of Shigella.	1.6/year	[14]
γ	Rate of (I) becoming asymptomatic infectious (C).	0.4/year	Assumed
ζ	Treatment rate for symptomatic infectious individuals.	0.4/year	Assumed
f	Proportion of latently infected humans who proceed to symptomatic infectious humans.	0.9	[12]
θ	Screening rate for asymptomatic infectious humans.	0.3/year	Assumed

3. Model formulation

The primary goal of this work is to construct a mathematical model that characterizes the dynamics of *Shigellosis* with the help of fractional order calculus in the Caputo sense. The model is built upon the research conducted by [14] and [42], and it has been upgraded by including the Caputo derivative notion. This includes hereditary traits, notably memory effects, that can modify the qualitative dynamics of *Shigellosis* infection. The model also includes two crucial control interventions: medical treatment and sanitation, which depict actual scenarios where managing infectious diseases typically entails a hybrid of medical treatment and sanitation measures. The total populace is sub-divided into five epidemiological groups: the at-risk, symptomatic (infectious and display symptoms), asymptomatic (infectious but do not show symptoms), and healed individuals denoted by $S(t)$, $E(t)$, $I(t)$, $A(t)$, and $R(t)$ respectively. The $SEIR$ model is improved by introducing an asymptomatic group and including an extra group, B(t), which denotes the pool of *Shigellosis* pathogens in the surroundings. A proportion f of the individuals who have been exposed proceed to the symptomatic infectious compartment at a rate of δ. In contrast, the remaining individuals progress to the asymptomatic infectious class similarly. *Shigellosis* is a lethal disease, causing those who are infected symptomatically and asymptomatically to have mortality rates of d_1 and d_2 accordingly. Symptomatic and asymptomatic persons discharge pathogens into the surroundings, with each group contributing at rates ϵ_1 and ϵ_2 accordingly. The parameter μ_b indicates the natural decline of pathogens, and χ defines the clearing away of pathogens due to sanitary activities. A complete, detailed list of parameters values employed in the compartmental framework is depicted in Table 1. The following assumptions are made in the model development:

- All the parameter values are assumed positive, while the variables are assumed non-negative.
- There is a constant influx of individuals into susceptible populations at a rate Λ.
- The exposed group can be split into two groups, namely symptomatic and asymptomatic infectious humans.
- Susceptible humans may acquire *Shigellosis* infections through personal contact or by consuming contaminated fecal matter from the surroundings. The force infection

$$\lambda(t) = \alpha_1 I(t) + \alpha_2 A(t) + \alpha_3 B(t), \tag{10}$$

  is designated to capture the overall transmission. Here, parameters α_i, for $i = 1, 2, 3$, represent transmission rates concerning symptomatic humans, asymptomatic humans, and the pathogens' density, respectively.
- *Shigellosis* confers temporal immunity that depreciates at the rate ϕ.
- Each individual in a population may experience natural mortality at the are μ.
- Symptomatic infectious individuals can be healed through treatment or natural immunity at the rate ζ and η_1, respectively.
- There is a possibility of symptomatic transmission to asymptomatic infectious individuals at some rate γ.
- Asymptomatic infectious individuals depend only on natural healing η_2.
- Screening helps to detect asymptomatic humans at the rate θ.
- Symptomatic infectious humans shed more pathogens into the environment than asymptomatic humans.

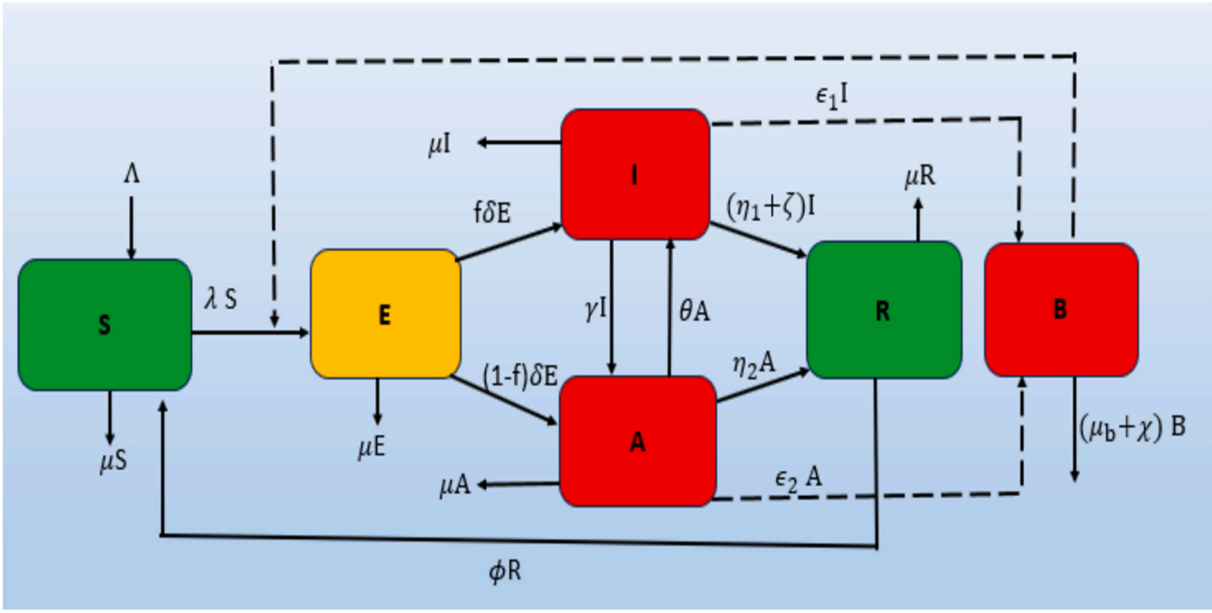

Fig. 1. The flow chart illustrates the transmission dynamics of *Shigellosis*, incorporating some control strategies.

From the above model details and assumptions, and with the aid of the flowchart given as Fig. 1, the deterministic model is presented as follows:

$$\begin{aligned}
\frac{dS}{dt} &= \Lambda + \phi R(t) - (\alpha_1 I(t) + \alpha_2 A(t) + \alpha_3 B(t) + \mu)S(t),\\
\frac{dE}{dt} &= (\alpha_1 I(t) + \alpha_2 A(t) + \alpha_3 B(t))S(t) - (\mu + \delta)E(t),\\
\frac{dI}{dt} &= f\delta E(t) + \theta A(t) - (\mu + d_1 + \eta_1 + \gamma + \zeta)I(t),\\
\frac{dC}{dt} &= (1-f)\delta E(t) + \gamma I(t) - (\mu + d_2 + \eta_2 + \theta)A(t),\\
\frac{dR}{dt} &= (\eta_1 + \zeta)I(t) + \eta_2 A(t) - (\mu + \phi)R(t),\\
\frac{dB}{dt} &= \epsilon_1 I(t) + \epsilon_2 A(t) - (\mu_b + \chi)B(t).
\end{aligned} \tag{11}$$

The initial conditions (ICs) for the model system (11) are

$$S(0) > 0, E(0) > 0, I(0) > 0, A(0) > 0, R(0) > 0, B(0) > 0. \tag{12}$$

Hence, the fractional order *Shigellosis* system with the same order is depicted as follows:

$$\begin{aligned}
{}_0^C D_t^\alpha S(t) &= \Lambda + \phi R(t) - (\alpha_1 I(t) + \alpha_2 A(t) + \alpha_3 B(t) + \mu)S(t),\\
{}_0^C D_t^\alpha E(t) &= (\alpha_1 I(t) + \alpha_2 A(t) + \alpha_3 B(t))S(t) - (\mu + \delta)E(t),\\
{}_0^C D_t^\alpha I(t) &= f\delta E(t) + \theta A(t) - (\mu + d_1 + \eta_1 + \gamma + \zeta)I(t),\\
{}_0^C D_t^\alpha A(t) &= (1-f)\delta E(t) + \gamma I(t) - (\mu + d_2 + \eta_2 + \theta)A(t),\\
{}_0^C D_t^\alpha R(t) &= (\eta_1 + \zeta)I(t) + \eta_2 A(t) - (\mu + \phi)R(t),\\
{}_0^C D_t^\alpha B(t) &= \epsilon_1 I(t) + \epsilon_2 A(t) - (\mu_b + \chi)B(t)
\end{aligned} \tag{13}$$

with the ICs as given in equation (12), where ${}_0^C D_t^\alpha$ means the Caputo FDE with $\alpha \in (0, 1)$.

The left-hand side (LHS) of the system (13) exhibits dimensions of $(time)^{-\alpha}$, which differs from the dimensions of the first-order ordinary system (13) whose RHS has a dimension $(time)^{-1}$. To ensure that the dimensions of both sides are equal, all non-negative parameters must be adjusted. The resulting version of the fractional system is provided as:

$$
\begin{aligned}
&{}_0^C D_t^\alpha S(t) = \Lambda^\alpha + \phi^\alpha R(t) - (\alpha_1^\alpha I(t) + \alpha_2^\alpha A(t) + \alpha_3^\alpha B(t) + \mu^\alpha)S(t),\\
&{}_0^C D_t^\alpha E(t) = (\alpha_1^\alpha I(t) + \alpha_2^\alpha A(t) + \alpha_3^\alpha B(t))S(t) - (\mu^\alpha + \delta^\alpha)E(t),\\
&{}_0^C D_t^\alpha I(t) = f\delta^\alpha E(t) + \theta^\alpha A(t) - (\mu^\alpha + d_1^\alpha + \eta_1^\alpha + \gamma^\alpha + \zeta^\alpha)I(t),\\
&{}_0^C D_t^\alpha A(t) = (1-f)\delta^\alpha E(t) + \gamma^\alpha I(t) - (\mu^\alpha + d_2^\alpha + \eta_2^\alpha + \theta^\alpha)A(t),\\
&{}_0^C D_t^\alpha R(t) = (\eta_1^\alpha + \zeta^\alpha)I(t) + \eta_2^\alpha A(t) - (\mu^\alpha + \phi^\alpha)R(t),\\
&{}_0^C D_t^\alpha B(t) = \epsilon_1^\alpha I(t) + \epsilon_2^\alpha A(t) - (\mu_b^\alpha + \chi^\alpha)B(t),
\end{aligned}
\tag{14}
$$

where the ICs are as given in equation (12).

4. Analysis of fractional order model

4.1. Positivity and boundedness of solutions

Now, to establish this main property (i.e. positivity of the solution), whenever the ICs and all parameters are assumed to be positive, we introduce the following Theorem and corollary (see [41]).

Corollary 2. *Let $f(t) \in C[t_0, T]$ and ${}_{t_0}^C D_t^\alpha f(t) \in C[t_0, T]$ for $0 < \alpha \leq 1$. It is obvious from Theorem 1 that if ${}_{t_0}^C D_t^\alpha f(t) \geq 0$, $\forall_t \in (t_0, T)$ then $f(t)$ is non-decreasing $\forall_t \in (t_0, T)$ and if ${}_{t_0}^C D_t^\alpha f(t) \leq 0$, $\forall_t \in (t_0, T)$ then $f(t)$ is non-increasing $\forall_t \in (t_0, T]$.*

Therefore, we can now state the following main theorem:

Theorem 3. *The region*

$$
\Pi_+ = \{S, E, I, A, R, B \geq 0 : S + E + I + A + R \leq \frac{\Lambda^\alpha}{\mu^\alpha}, B \leq \frac{(\epsilon_1^\alpha + \epsilon_2^\alpha)\Lambda^\alpha}{\mu^\alpha(\mu_b^\alpha + \chi^\alpha)}\},
\tag{15}
$$

is positive invariant set for the FOM (14).

Proof. The work by [45] guarantees the existence and uniqueness of the solution to the Fractional Order Model (FOM) (14) on the interval $(0, \infty)$. We shall now demonstrate that the region Π_+ for the FOM remains positive over time since

$$
\begin{aligned}
&{}_0^C D_t^\alpha S(t)|_{S=0} = \Lambda^\alpha > 0,\\
&{}_0^C D_t^\alpha E(t)|_{E=0} = 0,\\
&{}_0^C D_t^\alpha I(t)|_{I=0} = 0,\\
&{}_0^C D_t^\alpha A(t)|_{A=0} = 0,\\
&{}_0^C D_t^\alpha R(t)|_{R=0} = 0,\\
&{}_0^C D_t^\alpha B(t)|_{B=0} = 0.
\end{aligned}
\tag{16}
$$

Next, the boundedness of the solution is deduced by adding up individual equations of the system (14), yielding

$$
\begin{aligned}
{}_0^C D_t^\alpha N(t) =& \Lambda^\alpha - \mu^\alpha N(t) - d_1^\alpha I(t) - d_2^\alpha A(t)\\
\leq& \Lambda^\alpha - \mu^\alpha N(t).
\end{aligned}
\tag{17}
$$

One can obtain

$$
N(t) \leq \frac{\Lambda^\alpha}{\mu^\alpha} + (-\frac{\Lambda^\alpha}{\mu^\alpha} + N(0))E_\alpha(-\mu^\alpha t^\alpha),
\tag{18}
$$

where

$$
E_\alpha(z) = \sum_{k=0}^{\infty} \frac{z^k}{\Gamma(\alpha k + 1)},
$$

is the Mittag–Leffler function of parameter α (see Definition 4 at equation (8)). Therefore, by asymptotic behaviour of the Mittag–Leffler function [36,46], we obtain

$$N(t) \leq \frac{\Lambda^{\alpha}}{\mu^{\alpha}}. \tag{19}$$

Similarly, it can be verified from model (14) that get $B(t) \leq \frac{(\epsilon_1^{\alpha}+\epsilon_2^{\alpha})\Lambda^{\alpha}}{\mu^{\alpha}(\mu_b^{\alpha}+\chi^{\alpha})}$. Hence, the set Π_+ is a positive invariant region for the model (14). The result implies that the proposed model can be deemed epidemiologically valid, as it is mathematically well-defined and guarantees that all solutions of the *Shigellosis* model, when initialized, stay within the feasible zone Π_+. □

4.2. Existence and uniqueness of solutions

The proof for the existence and uniqueness of solutions for fractional order IVPS is customarily established via the fixed point theorems such as Picard's, Schauder and the Banach contraction mapping principle [60,62]. The current study will employ the Banach contraction principle to establish the main results. Let the FOM (14) in Caputo sense be written in the form:

$$ {}_0^C D_t^{\alpha} u(t) = \Omega(t, u(t)), \text{for} \quad t \geq 0, \text{with} \quad u(0) = u_0 \in \mathbb{R}_+, where \quad \Omega : \mathbb{R}_+ \times \mathbb{R}^6 \to \mathbb{R}, \tag{20}$$

Lemma 1. *Suppose* $\Omega(t, u(t))$ *holds for the conditions:*

1. Ω *is a continuous function with respect to* t *for every* $u(t) \in \mathbb{R}^n$,
2. Ω *and* $\frac{\partial \Omega}{\partial u}$ *are continuous functions with respect to* $u(t) \in \mathbb{R}^n$,
3. $\|\Omega\| \leq q_1 + q_2 \|u\|$ *for all* $u(t) \in \mathbb{R}^n$, *and all* $q_1, q_2 > 0$.

Therefore, FOM (14) *has a unique solution on the interval* $[0, +\infty)$.

Proof. Let FOM (14) be reformulated as

$$\begin{aligned} {}_0^C D_t^{\alpha} u(t) &= \Omega(t, u(t)), \text{for} \quad t \geq 0, \text{with} \quad u(0) = u_0 \in \mathbb{R}_+, where \quad \Omega : \mathbb{R}_+ \times \mathbb{R}^6 \to \mathbb{R}, \\ \Omega(t, u(t)) &= Q_2 + Q_1 u(t) + S(t)B(t)u(t), u(t) = (S(t), E(t), I(t), A(t), R(t), B(t))^T, \\ u_0 &= (\Lambda, 0, 0, 0, 0, 0)^T, \end{aligned} \tag{21}$$

where

$$Q_1 = \begin{bmatrix} -\mu^{\alpha} & 0 & 0 & 0 & \phi^{\alpha} & 0 \\ 0 & -w_0^{\alpha} & 0 & 0 & 0 & 0 \\ 0 & f\delta^{\alpha} & -w_1^{\alpha} & \theta^{\alpha} & 0 & 0 \\ 0 & (1-f)\delta^{\alpha} & \gamma^{\alpha} & -w_2^{\alpha} & 0 & 0 \\ 0 & 0 & \eta_1^{\alpha} + \zeta^{\alpha} & \eta_2^{\alpha} & -w_3{}^{\alpha} & 0 \\ 0 & 0 & \epsilon_1^{\alpha} & \epsilon_2^{\alpha} & 0 & -w_4^{\alpha} \end{bmatrix},$$

and

$$Q_2 = \begin{bmatrix} 0 & 0 & -\alpha_1^{\alpha} & -\alpha_2^{\alpha} & 0 & -\alpha_3^{\alpha} \\ 0 & 0 & \alpha_1^{\alpha} & \alpha_2^{\alpha} & 0 & \alpha_3^{\alpha} \\ 0 & 0 & 0 & 0 & 0 & 0 \\ 0 & 0 & 0 & 0 & 0 & 0 \\ 0 & 0 & 0 & 0 & 0 & 0 \\ 0 & 0 & 0 & 0 & 0 & 0 \end{bmatrix},$$

with

$$\begin{aligned} w_0^{\alpha} &= \mu^{\alpha} + \delta^{\alpha}, \\ w_1^{\alpha} &= \mu^{\alpha} + d_1^{\alpha} + \eta_1^{\alpha} + \gamma^{\alpha} + \zeta^{\alpha}, \\ w_2^{\alpha} &= \mu^{\alpha} + d_2^{\alpha} + \eta_2^{\alpha} + \theta^{\alpha}, \\ w_3^{\alpha} &= \mu^{\alpha} + \phi^{\alpha}, \\ w_4^{\alpha} &= \mu_b^{\alpha} + \chi^{\alpha}. \end{aligned} \tag{22}$$

It may be noted that the vector function $u(t)$ also satisfies the initial and secondary conditions specified in Lemma 1. Now, it is necessary to check the third criterion. Following consideration of system (21), one may deduce the following:

$$\|\Omega\| \leq q_1 + q_2 \|u\|, \tag{23}$$

where $q_1 = \|Q_2\|$ and $q_2 = \|Q_1\| + \|S\| \|B\|$. Therefore, the third criterion for Lemma 1 is verified. Hence, the system (21) has a unique solution on $[0, +\infty)$. The theorem implies that the governing fractional order model possesses some feasible solutions, which are also unique. □

4.3. Equilibrium solutions

This part intends to determine the presence of equilibria within the system. The equilibria will shed light on the presence or absence of the disease in the community. To figure out these equilibrium points, begin by setting the right-hand side (RHS) of the system (14) equal to zero, then solve the subsequent system:

$${}_0^C D_t^\alpha = {}_0^C D_t^\alpha E(t) = {}_0^C D_t^\alpha I(t) = {}_0^C D_t^\alpha A(t) = {}_0^C D_t^\alpha R(t) = {}_0^C D_t^\alpha B(t) = 0. \tag{24}$$

Thus, the endemic equilibrium points are

$$\begin{aligned}
E^* &= h_1^\alpha I^*, \\
A^* &= h_2^\alpha I^*, \\
R^* &= h_3^\alpha I^*, \\
S^* &= \frac{\Lambda^\alpha}{\mu^\alpha} + \left(\frac{\phi^\alpha h_3^\alpha}{\mu^\alpha} - \frac{(\mu^\alpha + \delta^\alpha) h_1^\alpha}{\mu^\alpha} \right) I^*, \\
B^* &= \left(\frac{\epsilon_1^\alpha + \epsilon_2^\alpha h_2^\alpha}{w_4^\alpha} \right) I^*,
\end{aligned} \tag{25}$$

where

$$\begin{aligned}
h_1^\alpha &= \frac{w_1^\alpha w_2^\alpha - \theta^\alpha \gamma^\alpha}{f\delta^\alpha w_2^\alpha + (1-f)\delta^\alpha \theta^\alpha}, \\
h_2^\alpha &= \frac{f\delta^\alpha + (1-f) w_1^\alpha \delta^\alpha}{f\delta^\alpha w_2^\alpha + (1-f)\delta^\alpha \theta^\alpha}, \\
h_3^\alpha &= \frac{\eta_1^\alpha + \zeta^\alpha + \eta_2^\alpha h_2^\alpha}{f\delta^\alpha w_2^\alpha + (1-f)\delta^\alpha \theta^\alpha}.
\end{aligned}$$

It can be noted that

$$\lambda^* = \alpha_1^\alpha I^* + \alpha_2^\alpha A^* + \alpha_3^\alpha B^* = h_4^\alpha I^*, \tag{26}$$

where

$$h_4^\alpha = \alpha_1^\alpha + \alpha_2^\alpha h_2^\alpha + \frac{\alpha_3^\alpha \left(\epsilon_1^\alpha + \epsilon_2^\alpha h_2^\alpha \right)}{w_4^\alpha}.$$

After some algebraic manipulations on equation (26), one can obtain

$$h_4^\alpha I^* \left(\frac{\Lambda^\alpha}{\mu^\alpha} + \left(\frac{\phi^\alpha h_3^\alpha}{\mu^\alpha} - \frac{(\mu^\alpha + \delta^\alpha) h_1^\alpha}{\mu^\alpha} \right) I^* \right) = (\mu^\alpha + \delta^\alpha) h_1^\alpha I^*. \tag{27}$$

Equation (27) has two solutions:

$$\begin{aligned}
I^* &= 0, \\
I^* &= \frac{\Lambda^\alpha}{\mu^\alpha + \delta^\alpha} + \frac{\phi^\alpha h_3^\alpha}{\mu^\alpha + \delta^\alpha} - \frac{1}{h_4^\alpha} = \frac{1}{h_4^\alpha} \left(\frac{h_4^\alpha (\Lambda^\alpha + \phi^\alpha h_3^\alpha)}{\mu^\alpha + \delta^\alpha} - 1 \right) = \frac{1}{h_4^\alpha} (R_e - 1),
\end{aligned} \tag{28}$$

where

$$R_e = \frac{h_4^\alpha (\Lambda^\alpha + \phi^\alpha h_3^\alpha)}{\mu^\alpha + \delta^\alpha}. \tag{29}$$

The findings suggest that whenever $I^* = 0$, there is a presence of disease-free equilibrium, but when $I^* = \frac{1}{h_4^\alpha}(R_e - 1)$, it signifies the presence of an endemic equilibrium point, which is only valid provided $R_e > 1$.

Shigellosis-Free Equilibrium Point (SFE)

In the absence of *Shigellosis* in the community, the infected class are considered to take no value (i.e. $I^* = A^* = E^* = 0$). Thus, the SFE is given by

$$E_0 = \left(\frac{\Lambda^\alpha}{\mu^\alpha}, 0, 0, 0, 0, 0 \right). \tag{30}$$

Shigellosis-endemic equilibrium Point

If *Shigellosis* prevails in the community, the equilibrium associated with its prevalence is known as the *Shigellosis*-endemic equilibrium point. It occurs when $S^*, E^*, I^*, A^*, R^*, B^*$ are all positive. To get the endemic equilibrium point in the current scenario, we substitute the value of $I^* = \frac{1}{h_4}(R_e - 1)$ into equation (25). It is clear that the endemic equilibrium persists provided $R_e > 1$.

4.4. The reproductive threshold and stability of equilibria

The effective reproduction number, typically referred to as R_e, is a fundamental metric in epidemiology. It quantifies the mean number of additional infections a particular person generates across the entire duration of their infectious period [47]. It plays a crucial role in forecasting and managing epidemics. The disease's chance of survivability or eradication inside a population depends on the value of R_e. This quantity also aids in the analysis of equilibrium stability.

If the value of R_e is less than 1, each infected individual causes fewer than one further infection, eventually eradicating the illness. On the other hand, if the reproductive number (R_e) is more than 1, each infected person spreads the disease to multiple individuals, spreading the infection across the community. A massive value of reproductive number (R_e) might suggest the likelihood of a substantial disease epidemic.

The calculation of R_e entails utilizing the next-generation matrix method, as delineated by [48]. The computation relies on identifying the maximum (dominant) eigenvalue, sometimes known as the spectral radius, of a matrix

$$FV^{-1} = \left[\frac{\partial \mathcal{F}_i(E_0)}{\partial x_j} \right] \left[\frac{\partial \mathcal{V}_i(E_0)}{\partial x_j} \right]^{-1}. \tag{31}$$

From system (14), one can deduce F and V as:

$$F = \begin{bmatrix} 0 & \alpha_1^\alpha S^0 & \alpha_2^\alpha S^0 & \alpha_3^\alpha S^0 \\ 0 & 0 & 0 & 0 \\ 0 & 0 & 0 & 0 \\ 0 & 0 & 0 & 0 \end{bmatrix},$$

$$V = \begin{bmatrix} w_0^\alpha & 0 & 0 & 0 \\ -f\delta^\alpha & w_1^\alpha & -\theta^\alpha & 0 \\ f-1 & -\gamma^\alpha & w_2^\alpha & 0 \\ 0 & -\epsilon_1^\alpha & -\epsilon_2^\alpha & w_4^\alpha \end{bmatrix},$$

then, the effective reproduction number is given by

$$R_e = \rho(FV^{-1}) = R_1 + R_2 + R_3, \tag{32}$$

where

$$R_1 = \frac{\left(f\delta^\alpha w_2^\alpha + (1-f)\theta^\alpha\right)\alpha_1^\alpha S^0}{\left(w_2^\alpha w_1^\alpha - \gamma^\alpha\theta^\alpha\right) w_0^\alpha},$$

$$R_2 = \frac{\left(w_1^\alpha(1-f) + \gamma^\alpha f\delta^\alpha\right)\alpha_2^\alpha S^0}{\left(w_2^\alpha w_1^\alpha - \gamma^\alpha\theta^\alpha\right) w_0^\alpha},$$

$$R_3 = \frac{\left(\epsilon_1^\alpha f\delta^\alpha w_2^\alpha + \epsilon_2^\alpha\gamma^\alpha f\delta^\alpha + (1-f)\left(\epsilon_1^\alpha\theta^\alpha + \epsilon_2^\alpha w_1^\alpha\right)\right)\alpha_3^\alpha S^0}{\left(w_2^\alpha w_1^\alpha - \gamma^\alpha\theta^\alpha\right) w_0^\alpha w_4^\alpha},$$

with w_0^α, w_1^α, w_2^α, and w_4^α defined in equation (22), whilst the expression for S^0 is given in equation (30). Furthermore, R_1, R_2 and R_3 represent the contribution of infections by symptomatic, asymptomatic infectives, and environmental pathogens, respectively.

4.5. Local stability of Shigellosis-free equilibrium

This entails the capability of the *Shigellosis* infection to return to its equilibrium after experiencing a small perturbation. This is done to ascertain long-term viability for SFE derived from equation (30). The next theorem clarifies this concept in a precise manner:

Theorem 4. *Consider the initial value problem (IVP)*

$${}_0^C D_t^\alpha u(t) = \Omega(t, u(t)), for \quad t \geq 0, with \quad u(0) = u_0 \in \mathbb{R}_+, where \quad \Omega : \mathbb{R}_+ \times \mathbb{R}_+^6 \to \mathbb{R}, 0 < \alpha \leq 1, \tag{33}$$

where ${}_0^C D_t^\alpha$ represents the time FDE in the Caputo sense, $\Omega : \mathbb{R}_+ \times \mathbb{R}^6 \to \mathbb{R}$ stands for a vector field. The DFE is locally asymptotically stable if all eigenvalues, λ_i, of the Jacobian matrix of $\Omega(t, u(t))$ at E_0 satisfy $\left|Arg(\lambda_i)\right| > \frac{\pi\alpha}{2}$, for $i = 1, 2, 3, 4, 5, 6$.

Proof. The Jacobian Matrix, denoted as J, is obtained by calculating the partial derivatives of the system (11) with respect to the state variables $(S(t), E(t), I(t), A(t), R(t), B(t))$ evaluated at E_0.

$$J(E_0) = \begin{bmatrix} -\mu^\alpha & 0 & -\alpha_1^\alpha S_0 & -\alpha_2^\alpha S_0 & \phi^\alpha & -\alpha_3^\alpha S_0 \\ 0 & -w_0^\alpha & \alpha_1^\alpha S_0 & \alpha_2^\alpha S_0 & 0 & \alpha_3^\alpha S_0 \\ 0 & \delta^\alpha & -w_1^\alpha & 0 & 0 & 0 \\ 0 & 0 & \gamma^\alpha & -w_2^\alpha & 0 & 0 \\ 0 & 0 & \eta_1^\alpha + \zeta^\alpha & \eta_2^\alpha & -w_3^\alpha & 0 \\ 0 & 0 & \epsilon_1^\alpha & \epsilon_2^\alpha & 0 & -w_4^\alpha \end{bmatrix} \tag{34}$$

with w_0^α, w_1^α, w_2^α, w_3^α, and w_4^α defined in equation (22).

Expression (34) yields the following eigenvalues: $\lambda = -\mu^\alpha$ and $\lambda = -w_3^\alpha$ which are always negative.

To work with the rest of the eigenvalues, it is vital to consider the remnant matrix denoted by J_1

$$J_1(E_0) = \begin{bmatrix} -Z_{11} & Z_{12} & Z_{13} & Z_{14} \\ Z_{21} & -Z_{22} & 0 & 0 \\ 0 & Z_{32} & -Z_{33} & 0 \\ 0 & Z_{42} & Z_{43} & -Z_{44} \end{bmatrix}, \tag{35}$$

where $Z_{11} = w_0^\alpha, Z_{12} = \alpha_1^\alpha S_0, Z_{13} = \alpha_2^\alpha S_0, Z_{14} = S_0\alpha_3^\alpha, Z_{21} = \delta^\alpha, Z_{22} = w_1^\alpha, Z_{32} = \gamma^\alpha,\ Z_{33} = w_2^\alpha, Z_{42} = \epsilon_1^\alpha, Z_{43} = \epsilon_2^\alpha, Z_{44} = w_4^\alpha$. From which, one can derive a polynomial of the form:

$$\lambda^4 + l_3\lambda^3 + l_2\lambda^2 + l_1\lambda + l_0 = 0, \tag{36}$$

where

$$\begin{aligned} l_3 =& Z_{11} + Z_{22} + Z_{33} + Z_{44}, \\ l_2 =& \left(Z_{44}Z_{33} + Z_{44}Z_{22} + Z_{44}Z_{11} + Z_{33}Z_{22} + Z_{33}Z_{11} + Z_{22}Z_{11}(1 - R_d)\right), \\ l_1 =& Z_{11}Z_{22}Z_{44}\left(1 - \left(R_a + R_d\right)\right) + Z_{11}Z_{22}Z_{33}\left(1 - \left(R_c + R_d\right)\right) \\ &+ Z_{22}Z_{33}Z_{44} + Z_{11}Z_{33}Z_{44}, \\ l_0 =& Z_{44}Z_{33}Z_{22}Z_{11}\left(1 - R_e\right). \end{aligned}$$

Note that R_e can be partitioned into four terms:

$$R_e = R_a + R_b + R_c + R_d, \tag{37}$$

where

$$R_a = \frac{Z_{43}Z_{32}Z_{21}Z_{14}}{Z_{44}Z_{33}Z_{22}Z_{11}},$$

$$R_b = \frac{Z_{42}Z_{21}Z_{14}Z_{33}}{Z_{44}Z_{33}Z_{22}Z_{11}},$$

$$R_c = \frac{Z_{44}Z_{32}Z_{21}Z_{13}}{Z_{44}Z_{33}Z_{22}Z_{11}},$$

$$R_d = \frac{Z_{44}Z_{33}Z_{21}Z_{12}}{Z_{44}Z_{33}Z_{22}Z_{11}}.$$

The Routh-Hurwitz stability criterion [49,50]) guarantees negativity of all the roots of equation (36) provided

$$l_3 > 0, l_2 > 0, l_1 > 0, l_0 > 0, \tag{38}$$

and

$$D_1 = l_3 > 0,$$
$$D_2 = \begin{vmatrix} l_3 & 1 \\ l_1 & l_2 \end{vmatrix} = l_3 l_2 - l_1 > 0,$$
$$D_3 = \begin{vmatrix} l_3 & 1 & 0 \\ l_1 & l_2 & l_3 \\ 0 & l_0 & l_1 \end{vmatrix} = l_1 l_2 l_3 - l_1^2 - l_0 l_3^2 > 0, \tag{39}$$
$$D_4 = \begin{vmatrix} l_3 & 1 & 0 & 0 \\ l_1 & l_2 & l_3 & 1 \\ 0 & l_0 & l_1 & l_2 \\ 0 & 0 & 0 & l_0 \end{vmatrix} = l_0 \left(l_1 l_2 l_3 - l_1^2 - l_0 l_3^2 \right) > 0.$$

It is clear that $D_1 = l_3 > 0$. Additionally, if $R_e < 1$, then $R_a, R_b, R_c, R_d < 1$ and hence $l_0, l_1, l_2 > 0$. Also, D_2 can be established positive as follows:

$$D_2 = (Z_{11} + Z_{22} + Z_{33} + Z_{44})(Z_{11}Z_{33} + Z_{11}Z_{44} + Z_{22}Z_{33} + Z_{22}Z_{44} + Z_{33}Z_{44} + Z_{11}Z_{22}(1 - R_d))$$
$$- Z_{11}Z_{33}Z_{44} - Z_{22}Z_{33}Z_{44} - Z_{11}Z_{22}Z_{44}(1 - R_a - R_d) - Z_{11}Z_{22}Z_{33}(1 - R_c - R_d).$$

The rest of the condition is to verify that

$$D_3 = l_1(l_2 l_3 - l_1) - l_0 l_3^2 > 0. \tag{40}$$

In order to prove the validity of the inequality (40), it is enough to show the following set of inequalities:

$$l_1 l_2 l_3 > 2l_1^2, \tag{41}$$
$$l_1 l_2 l_3 > 2l_0 l_3^2. \tag{42}$$

In order prove (41), express $l_2 l_3 - 2l_1$ as a combined total of the subsequent portions:

$$\begin{aligned} l_2 l_3 - 2l_1 =& Z_{11}Z_{33}^2 + Z_{11}^2 Z_{33} + Z_{11}Z_{44}^2 + Z_{22}Z_{33}^2 + Z_{11}^2 H44 \\ &+ Z_{22}^2 Z_{33} + Z_{22}H44^2 + Z_{22}^2 H44 + Z_{33}H44^2 + Z_{33}^2 H44 + Z_{11}Z_{22}Z_{33} + Z_{11}Z_{22}Z_{44} \\ &+ Z_{11}Z_{33}Z_{44} + Z_{22}Z_{33}Z_{44} + Z_{11}Z_{22}^2(1 - Rd) + Z_{11}^2 Z_{22}(1 - R_d) \\ &+ 2Z_{11}Z_{22}Z_{44}R_a + 2Z_{11}Z_{22}Z_{33}R_c + Z_{11}Z_{22}Z_{33}R_d + Z_{11}Z_{22}Z_{44}R_d. \end{aligned}$$

To prove equation (42), express $l_1 l_2 - 2l_0 l_3$ the summation of terms:

$$\begin{aligned} l_1 l_2 - 2l_0 l_3 =& Z_{11}Z_{33}^2 Z_{44}^2 + Z_{11}^2 Z_{33}Z_{44}^2 + Z_{11}^2 Z_{33}^2 Z_{44} + Z_{22}Z_{33}^2 Z_{44}^2 + Z_{22}^2 Z_{33}Z_{44}^2 + Z_{22}^2 Z_{33}^2 Z_{44} \\ &+ Z_{11}Z_{22}^2 Z_{44}^2(1 - R_a - R_d) + Z_{11}^2 Z_{22}Z_{44}^2(1 - R_a - R_d) \\ &+ Z_{11}^2 Z_{22}^2 Z_{44}(1 - R_a - 2R_d + R_a R_d + R_d^2) + Z_{11}Z_{22}^2 Z_{33}^2(1 - R_c) \\ &+ Z_{11}^2 Z_{22}Z_{33}^2(1 - R_c - R_d) + Z_{11}^2 Z_{22}^2 Z_{33}(1 - R_c - 2R_d + R_d^2 + R_c R_d) \\ &+ Z_{11}Z_{22}^2 Z_{33}^2(1 - R_c - R_d) + Z_{11}Z_{22}Z_{33}Z_{44}^2 + Z_{11}Z_{22}Z_{33}^2 Z_{44} + Z_{11}Z_{22}Z_{33}Z_{44}^2 R_a \\ &+ 2Z_{11}Z_{22}Z_{33}^2 Z_{44}R_a + Z_{11}Z_{22}^2 Z_{33}Z_{44}R_a + Z_{11}^2 Z_{22}Z_{33}Z_{44}R_a \\ &+ 2Z_{11}Z_{22}Z_{33}Z_{44}^2 R_b + 2Z_{11}Z_{22}Z_{33}^2 Z_{44}R_b + 2Z_{11}Z_{22}^2 Z_{33}Z_{44}R_b \\ &+ 2Z_{11}^2 Z_{22}Z_{33}Z_{44}R_b + 2Z_{11}Z_{22}Z_{33}Z_{44}^2 R_c + Z_{11}Z_{22}Z_{33}^2 Z_{44}R_c + Z_{11}Z_{22}^2 Z_{33}Z_{44}R_c \\ &+ Z_{11}^2 Z_{22}Z_{33}Z_{44}R_c + Z_{11}Z_{22}Z_{33}Z_{44}^2 R_d + Z_{11}Z_{22}Z_{33}^2 Z_{44}R_d \\ &+ Z_{11}Z_{22}^2 Z_{33}Z_{44}(1 - R_d) + Z_{11}^2 Z_{22}Z_{33}Z_{44}(1 - R_d) + Z_{11}^2 Z_{22}^2 Z_{44}R_a R_d. \end{aligned}$$

One can note that $l_1 l_2 - 2l_0 l_3 > 0$ and $l_2 l_3 - 2l_1 > 0$ so long $R_e < 1$ and each $R_a, R_b, R_c, R_d < 1$. Using the above results one can deduce that (41) and (42) are valid, the same applies for (40). Furthermore, the verification for condition D_4 may be derived from the equation $D_4 = l_0 D_3$. It has been established before that $D_3 > 0$, thus $D_4 = l_0 D_3 > 0$. Therefore, all the requirements of the Routh-Hurwitz criterion apply to this particular scenario (equations (38) and (39)), then the *Shigellosis*-free equilibrium E_0 is locally asymptotically stable whenever $R_e < 1$. □

4.6. Hyers–Ulam stability of Fractional Caputo FDEs

In this part, we establish the global stability of the Fractional Caputo FDEs (14) in the Hyers–Ulam stability sense. Before going further, consider some basic definitions needed to establish the main results. Consider the compact version of the FOM (14) in Caputo sense to be written as

$$ {}_0^C D_t^{\alpha} u(t) = \Omega(t, u(t)), \text{for} \quad t \geq 0, \text{with} \quad u(0) = u_0 \in \mathbb{R}_+, where \quad \Omega : \mathbb{R}_+ \times \mathbb{R}^6 \to \mathbb{R}, \tag{43} $$

where $u_0, u(t), \Omega(t, u(t))$ have been defined in equation (21). Consider the inequality:

$$ \left\| {}^C D_{0+}^{\alpha} u(t) - \Omega(t, u(t)) \right\|_1 < \epsilon, \quad \forall t \in [0, T]. \tag{44} $$

Definition 6. Now, $y \in \mathbb{E}$ is a solution of equation (43) if and only if there is a $h \in \mathbb{E}$ such that:

$$ |h(t)| \leq \epsilon, \text{where} \quad h = max(h_j)^T, j = 1, ...6, \forall t \in [0, T], \tag{45} $$

and

$$ {}^C D_{0+}^{\alpha} y(t) = \Omega(t, y(t)) + h(t), \forall t \in [0, T]. \tag{46} $$

Now, applying the fractional R-LF integral to both sides of (46) gives

$$ y(t) = y_0 + \frac{1}{\Gamma(\alpha)} \int_0^t (t - \tau)^{\alpha - 1} \Omega(\tau, y(\tau)) d\tau + \frac{1}{\Gamma(\alpha)} \int_0^t (t - \tau)^{\alpha - 1} h(\tau) d\tau. \tag{47} $$

Consider the expression

$$ \left\| y(t) - y_0 - \frac{1}{\Gamma(\alpha)} \int_0^t (t - \tau)^{\alpha - 1} \Omega(\tau, y(\tau)) d\tau \right\|_1. \tag{48} $$

Substitute the expression for $y(t)$ from equation (47) into equation (48) and applying condition (45) gives

$$ \begin{aligned} \left\| y(t) - y_0 - \frac{1}{\Gamma(\alpha)} \int_0^t (t - \tau)^{\alpha - 1} \Omega(\tau, y(\tau)) d\tau \right\|_1 &= \left| \frac{1}{\Gamma(\alpha)} \int_0^t (t - \tau)^{\alpha - 1} h(\tau) d\tau \right|, \\ &= \frac{1}{\Gamma(\alpha)} \int_0^t (t - \tau)^{\alpha - 1} |h(\tau)| \, d\tau, \\ &\leq \frac{\epsilon}{\Gamma(\alpha)} \int_0^t (t - \tau)^{\alpha - 1} d\tau, \\ &\leq \frac{\epsilon T^{\alpha}}{\Gamma(\alpha + 1)}. \end{aligned} \tag{49} $$

Therefore, we have

$$ \left\| y(t) - y_0 - \frac{1}{\Gamma(\alpha)} \int_0^t (t - \tau)^{\alpha - 1} \Omega(\tau, y(\tau)) d\tau \right\|_1 \leq \frac{\epsilon T^{\alpha}}{\Gamma(\alpha + 1)}, \quad \forall t \in [0, T]. \tag{50} $$

Definition 7. The *Shigellosis* model fractional model (43) is Ulam-Hyers stable on $[0, T]$ if there exists a constant $M > 0$, such that for every $\epsilon > 0$ and a solution $y \in \mathbb{E}$ satisfying (44) there exists a unique solution in $u \in \mathbb{E}$ of equation (43), with

$$ \|y(t) - u(t)\|_1 < M\epsilon, \quad \forall t \in [0, T], \text{where} \quad M = max(M_j)^T. \tag{51} $$

Theorem 5. *Suppose the assumptions in equations* (45) *and* (46) *of definition* (6) *hold. Then, the Shigellosis fractional model* (43) *is Ulam-Hyers stable on* $[0, T]$ *if*

$$ \Gamma(\alpha + 1) > \kappa T^{\alpha} \tag{52} $$

hold.

Proof. Recall Lemma 1, let u be a unique solution of the *Shigellosis* fractional model (43), take the R-LF integral to both sides of (46), we get

$$u(t) = u_0 + \frac{1}{\Gamma(\alpha)} \int_0^t (t-\tau)^{\alpha-1} \Omega(\tau, u(\tau)) d\tau. \tag{53}$$

Now, suppose $y_0 = u_0$, using equations (50) and (53), we compute $\|y(t) - u(t)\|_1$ as follows:

$$\|y(t) - u(t)\|_1 = \left\| y(t) - y_0 - \frac{1}{\Gamma(\alpha)} \int_0^t (t-\tau)^{\alpha-1} \Omega(\tau, u(\tau)) d\tau \right\|_1. \tag{54}$$

By adding and subtracting the term $\frac{1}{\Gamma(\alpha)} \int_0^t (t-\tau)^{\alpha-1} \Omega(\tau, y(\tau)) d\tau$ and applying the triangle inequality, we have

$$\begin{aligned} \|y(t) - u(t)\|_1 \leq & \left| y(t) - y_0 - \frac{1}{\Gamma(\alpha)} \int_0^t (t-\tau)^{\alpha-1} \Omega(\tau, y(\tau)) d\tau \right| \\ & + \left| \frac{1}{\Gamma(\alpha)} \int_0^t (t-\tau)^{\alpha-1} \Omega(\tau, y(\tau)) d\tau - \frac{1}{\Gamma(\alpha)} \int_0^t (t-\tau)^{\alpha-1} \Omega(\tau, u(\tau)) d\tau \right|. \end{aligned} \tag{55}$$

Using (50) and the norm properties, one can get

$$\|y(t) - u(t)\|_1 \leq \frac{\epsilon T^\alpha}{\Gamma(\alpha+1)} + \frac{1}{\Gamma(\alpha)} \int_0^t (t-\tau)^{\alpha-1} \left| \left(\Omega(\tau, y(\tau)) - \Omega(\tau, u(\tau)) \right) \right| d\tau. \tag{56}$$

Applying the Contraction Mapping Principle [62] as also used in [63] (Theorem 3.2), yields

$$\|y(t) - u(t)\|_1 \leq \frac{\epsilon T^\alpha}{\Gamma(\alpha+1)} + \frac{\kappa T^\alpha}{\Gamma(\alpha+1)} \|y(t) - u(t)\|_1. \tag{57}$$

Algebraic manipulation gives $\|y(t) - u(t)\|_1 \leq M\epsilon$ where $M = \frac{T^\alpha}{\Gamma(\alpha+1) - \kappa T^\alpha}$. Following Definition 7, $M > 0$, provided $\Gamma(\alpha+1) - \kappa T^\alpha > 0$, which implies $\Gamma(\alpha+1) > \kappa T^\alpha$. Hence, fractional model (43) is Hyers–Ulam is stable at $[0, T]$. □

5. Adam-Bashforth-Moulton predictor–corrector scheme for the SEIAR-B model

The ABM method is the predominant numerical approach for solving fractional-order initial value problems (IVPs). The preference for the Adams PECE method is owing to the benefits they offer: they require least functions evaluations, making it more efficient and reliable than the other methods, such as extrapolation methods. Using the Corrector Predictor technique, the double-step approach addresses error estimation limitations in one-step methods (e.g., Runge-Kutta). The Adams-Moulton technique, a key component of the Adams method, adjusts step sizes and method ordering to accommodate error control. This method outperforms one-step methods like the Milne method by reducing unnecessary computations and time, resulting in significant improvements in computational tasks compared to multi-step approaches (see [57,58] for details).

Now, let us examine the FDE:

$${}_0^C D_t^\alpha u_j(t) = \Omega_j(t, u_j(t)), \text{for} \quad t \geq 0, \text{with} \quad u_j^r(0) = u_{j0} \in \mathbb{R}_+, r = 0, 1, 2, ..., \alpha, j \in \mathbb{N}, \tag{58}$$

where the differential operator ${}^C D_t^\alpha$ is identical to the well-known Volterra integral equation in the Caputo sense. Thus, we have

$$u_j(t) = \sum_{n=0}^{\alpha-1} u_{j_o}^r \frac{t^n}{n!} + \frac{1}{\Gamma(\alpha)} \int_0^t (t-\epsilon)^{\alpha-1} \Omega_i(\epsilon, u_j(\epsilon)) d\epsilon, j \in \mathbb{N}. \tag{59}$$

Using the ABM-PECE scheme, we explore the numerical solution of a fractional order SEICR-B model with sanitation and treatment. The algorithm is described in the following manner.

Let $h = \frac{T}{\hat{m}}, t_n = nh, n = 0, 1, 2, ...\hat{m}$.

Define the Corrector formulae by:

$$\begin{cases} S_{n+1} = & S_0 + \frac{h^\alpha}{\Gamma(\alpha+2)}\Big(\Lambda^\alpha + \phi^\alpha R^p_{n+1} - \big((\alpha_1^\alpha I^p_{n+1} + \alpha_2^\alpha C^p_{n+1} + \alpha_3^\alpha B^p_{n+1}) + \mu^\alpha\big)S^p_{n+1}\Big) + \\ & \frac{h^\alpha}{\Gamma(\alpha+2)}\sum_{j=0}^{n}\alpha_{j,n+1}\Big(\Lambda^\alpha + \phi^\alpha R_j - \big((\alpha_1^\alpha I_j + \alpha_2^\alpha C_j + \alpha_3^\alpha B_j) + \mu^\alpha\big)S_j\Big), \\ E_{n+1} = & E_0 + \frac{h^\alpha}{\Gamma(\alpha+2)}\Big((\alpha_1^\alpha I^p_{n+1} + \alpha_2^\alpha C^p_{n+1} + \alpha_3^\alpha B^p_{n+1})S^p_{n+1} - (\mu^\alpha + \delta^\alpha)E^p_{n+1}\Big) + \\ & \frac{h^\alpha}{\Gamma(\alpha+2)}\sum_{j=0}^{n}\alpha_{j,n+1}\Big((\alpha_1^\alpha I_j + \alpha_2^\alpha C_j + \alpha_3^\alpha B_j)S_j - (\mu^\alpha + \delta^\alpha)E_j\Big), \\ I_{n+1} = & I_0 + \frac{h^\alpha}{\Gamma(\alpha+2)}\Big(f\delta^\alpha E^p_{n+1} + \theta^\alpha C^p_{n+1} - (\mu^\alpha + d_1^\alpha + \eta_1^\alpha + \gamma^\alpha + \zeta^\alpha)I^p_{n+1}\Big) + \\ & \frac{h^\alpha}{\Gamma(\alpha+2)}\sum_{j=0}^{n}\alpha_{j,n+1}\Big(f\delta^\alpha E_j + \theta^\alpha C_j - (\mu^\alpha + d_1^\alpha + \eta_1^\alpha + \gamma^\alpha + \zeta^\alpha)I_j\Big), \\ C_{n+1} = & C_0 + \frac{h^\alpha}{\Gamma(\alpha+2)}\Big((1-f)\delta^\alpha E^p_{n+1} + \gamma^\alpha I^p_{n+1} - (\mu^\alpha + d_2^\alpha + \eta_2^\alpha + \theta^\alpha)C^p_{n+1}\Big) \\ & \frac{h^\alpha}{\Gamma(\alpha+2)}\sum_{j=0}^{n}\alpha_{j,n+1}\Big((1-f)\delta^\alpha E_j + \gamma^\alpha I_j - (\mu^\alpha + d_2^\alpha + \eta_2^\alpha + \theta^\alpha)C_j\Big), \\ R_{n+1} = & R_0 + \frac{h^\alpha}{\Gamma(\alpha+2)}\Big((\eta_1^\alpha + \zeta^\alpha)I^p_{n+1} + \eta_2^\alpha C^p_{n+1} - (\mu^\alpha + \phi^\alpha)R^p_{n+1}\Big) + \\ & \frac{h^\alpha}{\Gamma(\alpha+2)}\sum_{j=0}^{n}\alpha_{j,n+1}\Big((\eta_1^\alpha + \zeta^\alpha)I_j + \eta_2^\alpha C_j - (\mu^\alpha + \phi^\alpha)R_j\Big), \\ B_{n+1} = & B_0 + \frac{h^\alpha}{\Gamma(\alpha+2)}\Big(\epsilon_1^\alpha I^p_{n+1} + \epsilon_2^\alpha C^p_{n+1} - (\mu_b^\alpha + \chi^\alpha)B^p_{n+1}\Big) + \\ & \frac{h^\alpha}{\Gamma(\alpha+2)}\sum_{j=0}^{n}\alpha_{j,n+1}\Big(\epsilon_1^\alpha I_j + \epsilon_2^\alpha C_j - (\mu_b^\alpha + \chi^\alpha)B_j\Big). \end{cases} \tag{60}$$

Predictor formulae:

$$\begin{cases} S^p_{n+1} = & S_0 + \frac{1}{\Gamma(\alpha)}\sum_{j=0}^{n}\Xi_{j,n+1}\Big(\Lambda^\alpha + \phi^\alpha R_j - \big((\alpha_1^\alpha I_j + \alpha_2^\alpha C_j + \alpha_3^\alpha B_j) + \mu^\alpha\big)S_j\Big), \\ E^p_{n+1} = & E_0 + \frac{1}{\Gamma(\alpha)}\sum_{j=0}^{n}\Xi_{j,n+1}\Big((\alpha_1^\alpha I_j + \alpha_2^\alpha C_j + \alpha_3^\alpha B_j)S_j - (\mu^\alpha + \delta^\alpha)E_j\Big) \\ I^p_{n+1} = & I_0 + \frac{1}{\Gamma(\alpha)}\sum_{j=0}^{n}\Xi_{j,n+1}\Big(f\delta^\alpha E_j + \theta^\alpha C_j - (\mu^\alpha + d_1^\alpha + \eta_1^\alpha + \gamma^\alpha + \zeta^\alpha)I_j\Big), \\ C^p_{n+1} = & C_0 + \frac{1}{\Gamma(\alpha)}\sum_{j=0}^{n}\Xi_{j,n+1}\Big((1-f)\delta^\alpha E_j + \gamma^\alpha I_j - (\mu^\alpha + d_2^\alpha + \eta_2^\alpha + \theta^\alpha)C_j\Big), \\ R^p_{n+1} = & R_0 + \frac{1}{\Gamma(\alpha)}\sum_{j=0}^{n}\Xi_{j,n+1}\Big((\eta_1^\alpha + \zeta^\alpha)I_j + \eta_2^\alpha C_j - (\mu^\alpha + \phi^\alpha)R_j\Big), \\ B^p_{n+1} = & B_0 + \frac{1}{\Gamma(\alpha)}\sum_{j=0}^{n}\Xi_{j,n+1}\Big(\epsilon_1^\alpha I_j + \epsilon_2^\alpha C_j - (\mu_b^\alpha + \chi^\alpha)B_j\Big), \end{cases} \tag{61}$$

where

$$\alpha_{j,n+1} = \begin{cases} n^{\alpha+1} - (n-\alpha)(n+1)^\alpha, \text{if} \quad j = 0, \\ (n-j+2)^{\alpha+1} + (n-j)^{\alpha+1} - 2(n-j+1)^{\alpha+1}, \text{if} \quad 0 \le j \le n, \\ 1, \text{if} \quad j = 1, \end{cases}$$

and

$$\Xi_{j,n+1} = \frac{h^\alpha}{\alpha}\big((n+1-j)^\alpha - (n-j)^\alpha\big), 0 \le j \le n.$$

6. Numerical results and discussions

The fractional order model (11) was numerically solved in this part using the PECE approach of Adams–Bashforth–Moulton. The implementation was done in MATLAB. Multiple graphical representations (refer to Figs. 2 (a)-(f)) are provided and analyzed to confirm the previously stated analytical findings. The baseline values of parameters from Table 1 are utilized to facilitate simulations. The starting values for sub-populations were as follows: $S(0) = 60, E(0) = 40, I(0) = 20, A(0) = 90, R(0) = 20, B(0) = 500$ as given by Mwaijande and Mpogolo (2022, Preprint) [61]. This model system's fractional order α is selected from 0.75 to 1, inclusive.

6.1. Effects of memory on epidemic classes

To get a clear picture of the notion of memory effect, it is better to spell out this concept in terms of order of derivative α in the interval $0 < \alpha \le 1$. If the choice of order of the derivative is $\alpha = 1$, then there is no memory in the system (memoryless); the referred case is the classical calculus (integer order calculus). However, as α decreases from 1 through 0 exclusive, the level of memory increases. Therefore, the memory effect becomes negligible as α is so close to the unit. However, the memory effect increases as α diverges from the unit. Now, Fig. 2 (a)-(f) depicts the dynamics of all compartments as the fractional order α varies from 0.75

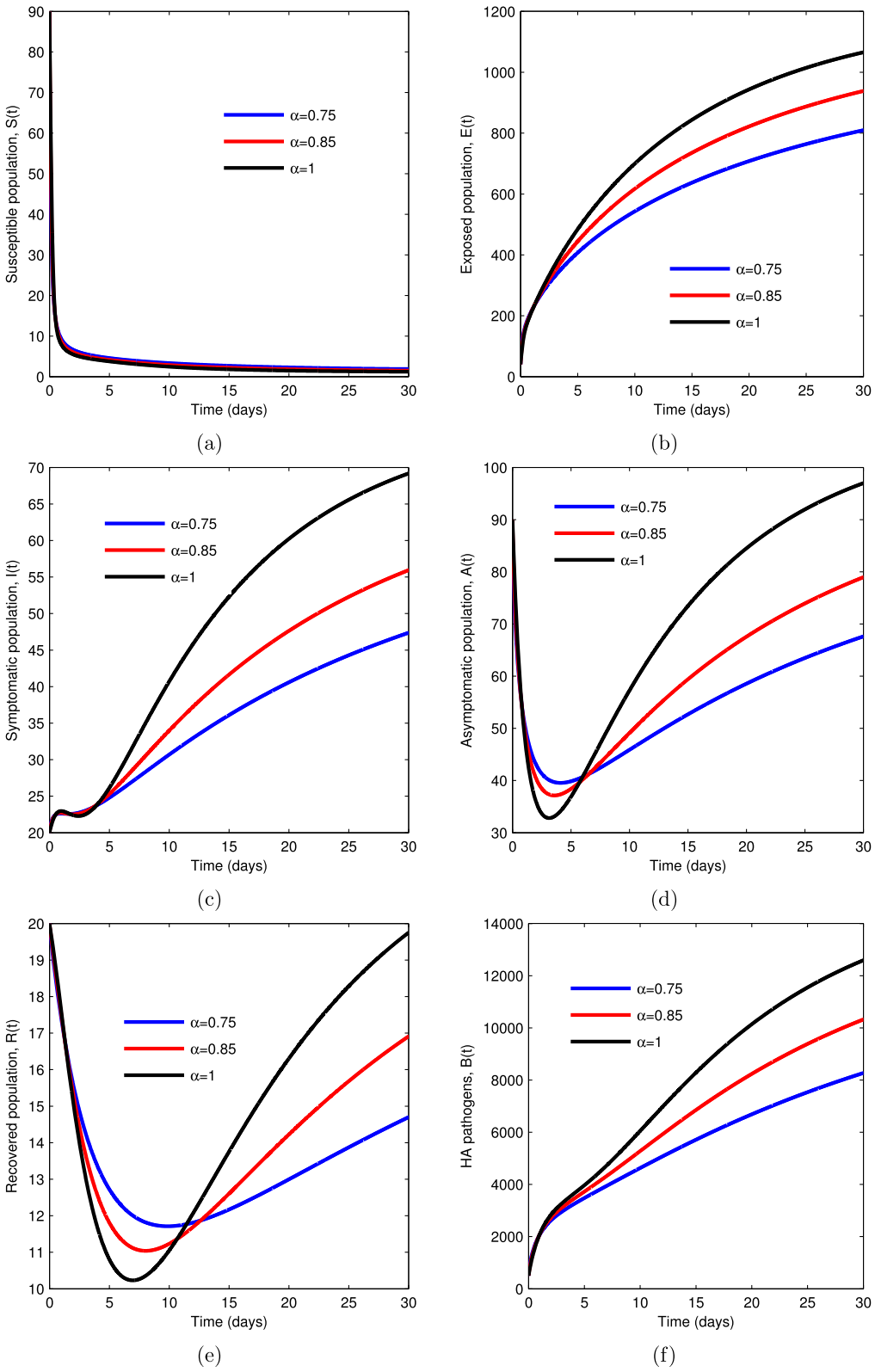

Fig. 2. (a)-(f) Show the impact of variation of memory parameter ($\alpha = 0.75, \alpha = 0.85$, and $\alpha = 1$) on different epidemiological classes (S, E, I, C, R, B).

through 1. In particular, Fig. 2(a) shows that the susceptible population increases with an increase in memory from 1 to 0.75. Fig. 2 (b) shows that with an increase in memory, there is a decrease in the exposed population. Also, Fig. 2 (c) shows that the population of symptomatic decreases with an increase in memory. The same applies to Fig. 2 (d), where the asymptomatic population decreases with similar reasoning. Also, Fig. 2 (e) shows that the population of recovered individuals increases with an increase in memory. Lastly, Fig. 2 (f) depicts that the population of *Shigellosis* pathogens increase when memory is deficient. The above findings imply that incorporating the memory effect (α) significantly reduces the size of disease cases. This has been witnessed in all disease classes see Figs. 2 (b)-(e). Nevertheless, when there is no memory ($\alpha = 1$) under the same circumstances, a high number of cases are observed because individuals are unaware of the previous strategies to contain an epidemic. Our findings also agree with other scholars such as [19,56,59].

6.2. Effects of control measures at a fixed fractional order

Fig. 3 (a)-(f) demonstrates the dynamical behaviour of all compartments, i.e. S, E, I, A, R and B when the treatment rate ζ is varied at the fixed fractional order $\alpha = 0.75$. This means eliminating the disease outbreak is more likely when the infected cases receive medical care. On the other hand, Fig. 4 (a)-(b) shows the impact of variation of sanitation measures (χ) on the dynamics of symptomatic humans and pathogens population. The numerical findings show a neglible effect on symptomatic humans as it is for the other classes not shown here for the purpose of being concise, but the effect is so evident in the pathogens population.

6.3. Impact of variation of contact rates and control measure parameters on the effective reproduction number (R_e)

It can be visualized from Fig. 5 (a)-(c) that the contact rates α_1, α_2, and α_3 influence the effective reproduction number R_e. An increase or decrease in contact rate, say α_1, α_2, α_3 or their combinations tend to increase or decrease R_e. Thus, the disease growth or decline of the outbreak depends on the nature of contact between the susceptible and infected populations and contact with contaminated food or water. This implies that it is imperative to minimize unnecessary contact with infected individuals to manage *Shigellosis* in the community. Furthermore, Fig. 5 (d) shows that an increase in sanitation parameter (χ) or treatment parameter (ζ) tends to decrease the effective reproduction number R_e. This implies that these control parameters are reasonably chosen for mitigating *Shigellosis* epidemic. Thus, to control *Shigellosis*, the government must increase the rate of treating already infected humans and ensure that the populace acquires services such as safe drinking water supply, sanitation and hygiene facilities.

7. Conclusions

This paper presents a unique and innovative approach to studying *Shigellosis* dynamics. It does so by introducing a fractional-order differential equation in the Caputo sense, a method that has not been widely explored in this context. Fundamental concepts of fractional calculus were presented to build a solid foundation for the findings. The relevant theorems concerning the *Shigellosis* model were established and proved. Qualitative features such as solutions' existence, uniqueness, and boundedness were thoroughly investigated. Moreover, stability analyses were conducted, encompassing both local stability, assessed through Routh's and global stability investigated through the Ulam-Hyers stability criteria. Numerical results were obtained using the predict-evaluate-correct-evaluate method of Adams–Bashforth–Moulton. The findings underscored the efficacy of routine therapies and sanitation practices for slowing the transmission of *Shigellosis* and decreasing the number of patients. The study also explored the influence of memory on *Shigellosis* dynamics by varying the fractional order within the range of 0.75 to 1. Results suggested that the increased memory effect led to a significant decline in disease incidence. These findings have significant practical implications. They highlight how understanding past disease prevalence and the effectiveness of countermeasures can profoundly influence our approach to the current situation. Future studies on *Shigellosis* might explore other fractional calculus derivatives such as Antagana-Baleanu, Riemann-Liouville, and Caputo-Fabrizio fractional, considering the limitations of Caputo derivatives in demanding higher conditions of regularity for differentiability as pointed out by [55]. One of our study's limitations is the lack of data to validate our conclusions. For this case, we utilized simulated data obtained from prior research. Undoubtedly, acquiring authentic data would enable us to get more exciting results than our current findings. Another aspect where future work could be directed is the incorporation of optimal control and cost-effectiveness in the present work. Despite the pitfalls, this work is an improvement of the classical models presented in literature regarding *Shigellosis* dynamics, where nonlocal features and memory effects were ignored. Eventually, the current work could still be helpful as it offers valuable insights for policymakers on successful strategies for controlling *Shigellosis* in the community.

Funding

This work did not receive any financial grants.

CRediT authorship contribution statement

Stephen Edward: Data curation, Formal analysis, Methodology, Software, Validation, Visualization, Writing – original draft, Writing – review & editing.

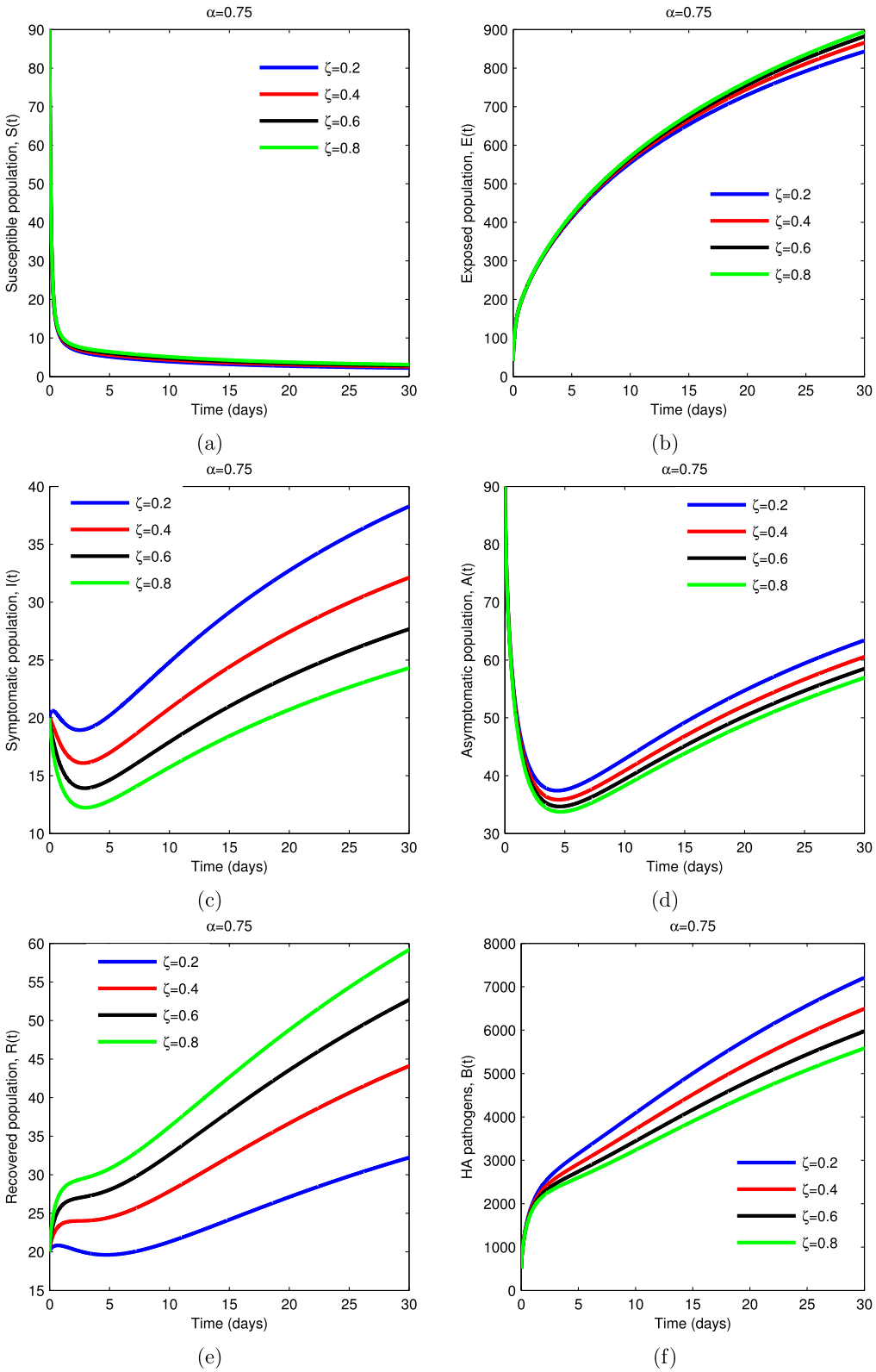

Fig. 3. (a)-(f) Show effects of variation of treatment parameter ζ, on different epidemiological classes (S, E, I, C, R, B): $\zeta = 0.2, \zeta = 0.4, \zeta = 0.6$ and $\zeta = 0.8$ at a fixed fractional order $\alpha = 0.75$.

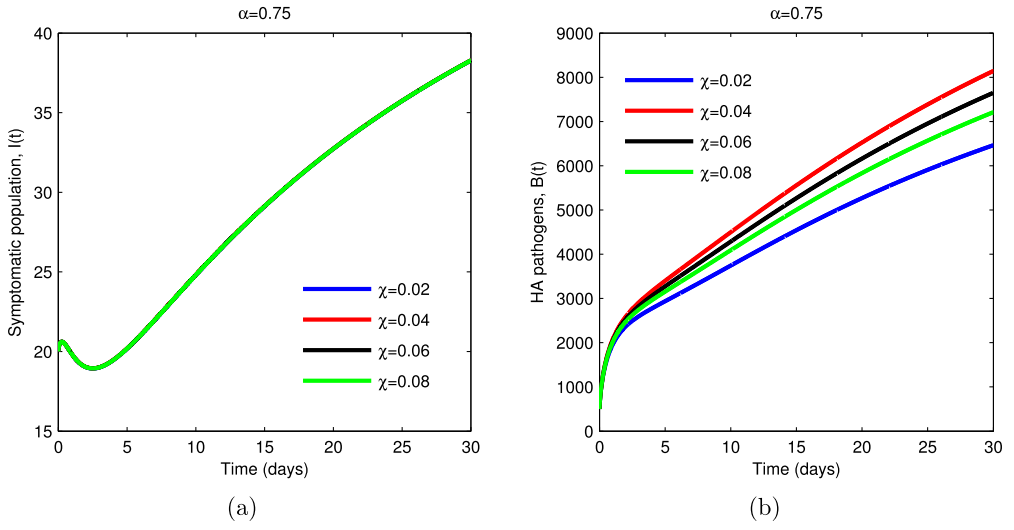

Fig. 4. (a)-(b) Show effects of variation of sanitation parameter χ, on different epidemiological classes (I, B): $\chi = 0.02, \chi = 0.04, \chi = 0.06$ and $\chi = 0.08$ at a fixed fractional order $\alpha = 0.75$.

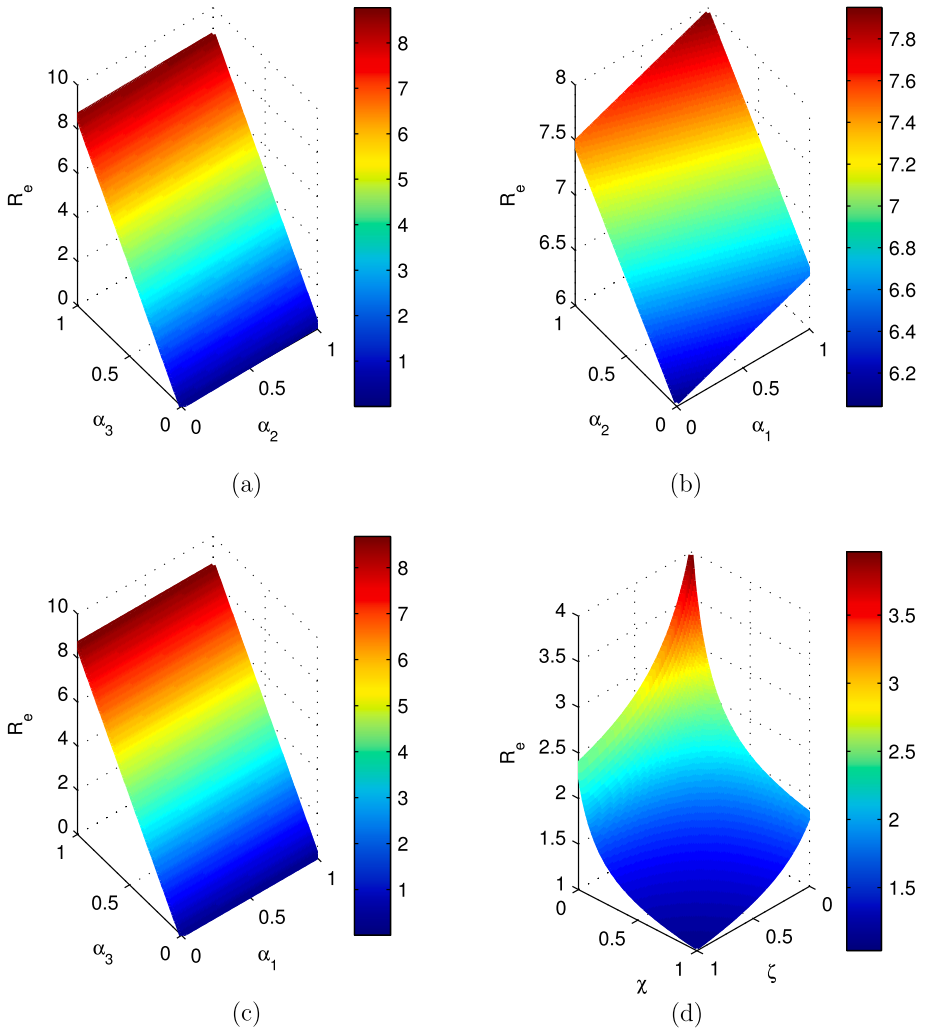

Fig. 5. (a)-(c) Depicts the impact contact rates $(\alpha_1, \alpha_2, \alpha_3)$ on the effective reproductive number R_e. Fig. 5(d) Shows the impacts of variation of χ and ζ on R_e.

Declaration of competing interest

The author declares that he has no competing interests.

Data availability

All the data and materials that support the findings of this study are included in the paper.

Acknowledgements

SE would like to appreciate the support received from the University of Dodoma during the preparation of this work.

References

[1] G.N. Schroeder, H. Hilbi, Molecular pathogenesis of Shigella spp.: controlling host cell signalling, invasion, and death by type III secretion, Clin. Microbiol. Rev. 21 (1) (2008) 134–156.
[2] K.L. Kotloff, J.P. Winickoff, B. Ivanoff, J.D. Clemens, D.L. Swerdlow, P.J. Sansonetti, G.K. Adak, M.M. Levine, Global burden of Shigella infections: implications for vaccine development and implementation of control strategies, Bull. World Health Organ. 77 (8) (1999) 651.
[3] Centers for Disease Control and Prevention (CDC), Shigella flexneri serotype 3 infections among men who have sex with men-Chicago, Illinois, 2003-2004, MMWR, Morb. Mort. Wkly. Rep. 54 (33) (2005) 820–822.
[4] A. Bowen, D. Eikmeier, P. Talley, A. Siston, S. Smith, J. Hurd, K. Smith, F. Leano, A. Bicknese, J.C. Norton, D. Campbell, Outbreaks of Shigella sonnei infection with decreased susceptibility to azithromycin among men who have sex with men—Chicago and metropolitan Minneapolis-St. Paul, 2014, Morb. Mort. Wkly. Rep. 64 (21) (2015) 597.
[5] A.A. Lindberg, P.D. Cam, N. Chan, L.K. Phu, D.D. Trach, G. Lindberg, K. Karlsson, A. Kärnell, E. Ekwail, Shigellosis in Vietnam: seroepidemiologic studies with the use of lipopolysaccharide antigens in enzyme immunoassays, Rev. Infect. Dis. 13 (Supplement-4) (1991) S231–S237.
[6] G.M. Garrity, D.J. Brenner, N.R. Krieg, J.R. Staley, B.S. Manual, Systematic bacteriology, in: The Proteobacteria, Part C: The Alpha-, Beta-, Delta-, and Epsilon-proteobacteria, Bergey's Manual Trust, vol. 2, Department of Microbiology and Molecular Genetics, 2005.
[7] F. He, K. Han, L. Liu, W. Sun, L. Zhang, B. Zhu, H. Ma, Shigellosis outbreak associated with contaminated well water in a rural elementary school: Sichuan Province, China, June 7-16, 2009, 2012.
[8] K.A. Lampel, S.B. Formal, A.T. Maurelli, A brief history of Shigella, EcoSal Plus 8 (1) (2018) 10–1128.
[9] M.M. Levine, K.L. Kotloff, E.M. Barry, M.F. Pasetti, M.B. Sztein, Clinical trials of Shigella vaccines: two steps forward and one step back on a long, hard road, Nat. Rev. Microbiol. 5 (7) (2007) 540–553.
[10] A. Phalipon, C. Costachel, C. Grandjean, A. Thuizat, C. Guerreiro, M. Tanguy, F. Nato, V.L. Normand, F. Bélot, K. Wright, V. Marcel-Peyre, Characterization of functional oligosaccharide mimics of the Shigella flexneri serotype 2a O-antigen: implications for the development of a chemically defined glycoconjugate vaccine, J. Immunol. 176 (3) (2006) 1686–1694.
[11] O. Chaturvedi, T. Masupe, S. Masupe, A continuous mathematical model for Shigella outbreaks, 2014.
[12] T. Chen, R.K.K. Leung, Z. Zhou, R. Liu, X. Zhang, L. Zhang, Investigation of key interventions for shigellosis outbreak control in China, PLoS ONE 9 (4) (2014) e95006.
[13] H.W. Berhe, O.D. Makinde, D.M. Theuri, Parameter estimation and sensitivity analysis of dysentery diarrhea epidemic model, J. Appl. Math. 2019 (2019).
[14] S. Edward, E. Mureithi, N. Shaban, Shigellosis dynamics: modelling the effects of treatment, sanitation, and education in the presence of carriers, Int. J. Math. Math. Sci. 2020 (2020).
[15] S. Edward, N. Shaban, E. Mureithi, Optimal control of shigellosis with cost-effective strategies, Comput. Math. Methods Med. 2020 (2020).
[16] S. Ullah, G. Zaman, Fractional order mathematical modeling and analysis of multi-infectious disease, 2023.
[17] R.M. Yulmetyev, N.A. Emelyanova, S.A. Demin, F.M. Gafarov, P. Hänggi, D.G. Yulmetyeva, Non-Markov stochastic dynamics of the real epidemic process of respiratory infections, Physica A, Stat. Mech. Appl. 331 (1–2) (2004) 300–318.
[18] S.P. Blythe, R.M. Anderson, Variable infectiousness in HFV transmission models, Math. Med. Biol., J. IMA 5 (3) (1988) 181–200.
[19] M. Saeedian, M. Khalighi, N. Azimi-Tafreshi, G.R. Jafari, M. Ausloos, Memory effects on epidemic evolution: the susceptible-infected-recovered epidemic model, Phys. Rev. E 95 (2) (2017) 022409.
[20] B.S.T. Alkahtani, A. Atangana, I. Koca, Huge analysis of the Hepatitis C model within the scope of fractional calculus, J. Nonlinear Sci. Appl. 9 (12) (2016) 6195–6203.
[21] A. Atangana, J.F. Gómez-Aguilar, Hyperchaotic behaviour obtained via a nonlocal operator with exponential decay and Mittag-Leffler laws, Chaos Solitons Fractals 102 (2017) 285–294.
[22] A. Atangana, I. Koca, Chaos in a simple nonlinear system with Atangana–Baleanu derivatives with fractional order, Chaos Solitons Fractals 89 (2016) 447–454.
[23] A.A.M. Arafa, S.Z. Rida, M. Khalil, The effect of anti-viral drug treatment of human immunodeficiency virus type 1 (HIV-1) is described by a fractional order model, Appl. Math. Model. 37 (4) (2013) 2189–2196.
[24] K.M. Owolabi, A. Atangana, Chaotic behaviour in a system of noninteger-order ordinary differential equations, Chaos Solitons Fractals 115 (2018) 362–370.
[25] K. Diethelm, A fractional calculus-based model for the simulation of an outbreak of dengue fever, Nonlinear Dyn. 71 (2013) 613–619.
[26] Y. Ding, H. Ye, A fractional-order differential equation model of HIV infection of CD4+ T-cells, Math. Comput. Model. 50 (3–4) (2009) 386–392.
[27] J.E. Escalante-Martínez, J.F. Gómez-Aguilar, C. Calderón-Ramón, A. Aguilar-Meléndez, P. Padilla-Longoria, A mathematical model of circadian rhythms synchronization using fractional differential equations system of coupled van der Pol oscillators, Int. J. Biomath. 11 (01) (2018) 1850014.
[28] J.E. Escalante-Martínez, J.F. Gómez-Aguilar, C. Calderón-Ramón, A. Aguilar-Meléndez, P. Padilla-Longoria, Synchronized bioluminescence behavior of a set of fireflies involving fractional operators of Liouville–Caputo type, Int. J. Biomath. 11 (03) (2018) 1850041.
[29] J.F. Gómez-Aguilar, A. Atangana, Fractional derivatives with the power-law and the Mittag–Leffler kernel applied to the nonlinear Baggs–Freedman model, Fractal Fract. 2 (1) (2018) 10.
[30] C.D.K. Bansi, C.B. Tabi, T.G. Motsumi, A. Mohamadou, Fractional blood flow in oscillatory arteries with thermal radiation and magnetic field effects, J. Magn. Magn. Mater. 456 (2018) 38–45.
[31] I. Ahmed, I.A. Baba, A. Yusuf, P. Kumam, W. Kumam, Analysis of Caputo fractional-order model for COVID-19 with lockdown, Adv. Differ. Equ. 2020 (1) (2020) 394.
[32] M. Rahman, M. Arfan, K. Shah, J.F. Gómez-Aguilar, Investigating a nonlinear dynamical model of COVID-19 disease under fuzzy Caputo, random and ABC, Chaos Solitons Fractals 140 (2020) 110232.
[33] J.F. Gómez-Aguilar, H. Yépez-Martínez, R.F. Escobar-Jiménez, C.M. Astorga-Zaragoza, J. Reyes-Reyes, Analytical and numerical solutions of electrical circuits described by fractional derivatives, Appl. Math. Model. 40 (21–22) (2016) 9079–9094.

[34] J.F. Gómez-Aguilar, B. Dumitru, Fractional transmission line with losses, Z. Naturforsch. A 69 (10–11) (2014) 539–546.
[35] V.F. Morales-Delgado, J.F. Gómez-Aguilar, M.A. Taneco-Hernández, R.F. Escobar-Jiménez, Fractional operator without singular kernel: applications to linear electrical circuits, Int. J. Circuit Theory Appl. 46 (12) (2018) 2394–2419.
[36] A.A. Kilbas, H.M. Srivastava, J.J. Trujillo, Theory and Applications of Fractional Differential Equations, vol. 204, Elsevier, 2006.
[37] M. Caputo, M. Fabrizio, A new definition of fractional derivative without singular kernel, Prog. Fract. Differ. Appl. 1 (2) (2015) 73–85.
[38] A. Atangana, D. Baleanu, New fractional derivatives with nonlocal and nonsingular kernel: theory and application to heat transfer model, arXiv preprint, arXiv:1602.03408, 2016.
[39] P. Anbalagan, R. Ramachandran, E. Hincal, Finite time synchronization of discontinuous fractional order Cohen–Grossberg memristive neural networks with discrete delays under sliding mode control strategies, in: Fractional-Order Modeling of Dynamic Systems with Applications in Optimization, Signal Processing and Control, Academic Press, 2022, pp. 213–248.
[40] I. Petras, Fractional-Order Nonlinear Systems: Modelling, Analysis and Simulation, Springer Science & Business Media, 2011.
[41] Z.M. Odibat, N.T. Shawagfeh, Generalized Taylor's formula, Appl. Math. Comput. 186 (1) (2007) 286–293.
[42] S. Edward, G.E. Mpogolo, Modeling and optimal control of the transmission dynamics of amebiasis, Results Control Optim. 13 (2023) 100325.
[43] J.H. Tien, D.J. Earn, Multiple transmission pathways and disease dynamics in a waterborne pathogen model, Bull. Math. Biol. 72 (2010) 1506–1533.
[44] M.J. Keeling, P. Rohani, Modeling Infectious Diseases in Humans and Animals, Princeton Univ., Princeton, NJ, 2008.
[45] W. Lin, Global existence theory and chaos control of fractional differential equations, J. Math. Anal. Appl. 332 (2007) 709–726.
[46] H.M. Srivastava, Fractional-order derivatives and integrals: introductory overview and recent developments, Kyungpook Math. J. 60 (1) (2020) 73–116.
[47] O. Diekmann, J.A.P. Heesterbeek, M.G. Roberts, The construction of next-generation matrices for compartmental epidemic models, J. R. Soc. Interface 7 (47) (2009) 873–885.
[48] P.V.D. Driessche, J. Watmough, Further notes on the basic reproduction number, in: Mathematical Epidemiology, Springer, Berlin, Heidelberg, 2008, pp. 159–178.
[49] E.X. DeJesus, C. Kaufman, Routh-Hurwitz criterion in the examination of eigenvalues of a system of nonlinear ordinary differential equations, Phys. Rev. A 35 (12) (1987) 5288.
[50] J. Morris, The Routh and Routh-Hurwitz stability criteria: their derivation by a novel method using comparatively elementary algebra, Aircr. Eng. Aerosp. Technol. 34 (1) (1962) 25–27.
[51] J.K.K. Asamoah, A fractional mathematical model of heartwater transmission dynamics considering nymph and adult amblyomma ticks, Chaos Solitons Fractals 174 (2023) 113905.
[52] J.K.K. Asamoah, G.Q. Sun, Fractional Caputo and sensitivity heat map for a gonorrhea transmission model in a sex structured population, Chaos Solitons Fractals 175 (2023) 114026.
[53] J.K.K. Asamoah, Fractal–fractional model and numerical scheme based on Newton polynomial for Q fever disease under Atangana–Baleanu derivative, Results Phys. 34 (2022) 105189.
[54] J.K.K. Asamoah, E. Okyere, E. Yankson, A.A. Opoku, A. Adom-Konadu, E. Acheampong, Y.D. Arthur, Non-fractional and fractional mathematical analysis and simulations for Q fever, Chaos Solitons Fractals 156 (2022) 111821.
[55] X.J. Yang, General Fractional Derivatives: Theory, Methods and Applications, Chapman and Hall/CRC, 2019.
[56] S.C. Mpeshe, Fractional-order derivative model of Rift Valley fever in urban peridomestic cycle, Discrete Dyn. Nat. Soc. 2021 (2021) 1–11.
[57] Lingbo Zhang, Studying and comparing numerical methods for ordinary differential equations, 2015.
[58] G. Polla, Comparing accuracy of differential equation results between Runge-Kutta Fehlberg methods and Adams-Moulton methods, Appl. Math. Sci. 7 (2013) 5115–5127.
[59] C.T. Deressa, G.F. Duressa, Analysis of Atangana–Baleanu fractional-order SEAIR epidemic model with optimal control, Adv. Differ. Equ. 2021 (2021) 1–25.
[60] S. Abbas, Existence of solutions to fractional order ordinary and delay differential equations and applications, Electron. J. Differ. Equ. 9 (2011) 1–11, available at: https://ejde.math.txstate.edu/Volumes/2011/09/abbas.pdf.
[61] S.E. Mwaijande, G.E. Mpogolo, Mathematical modeling of the transmission dynamics of amoebiasis with some interventions, preprint, available at: https://doi.org/10.21203/rs.3.rs-1363033/v1. (Accessed 5 May 2024), 2022.
[62] S. Banach, Sur les opérations dans les ensembles abstraits et leur application aux équations intégrales, Fundam. Math. 3 (1) (1922) 133–181.
[63] S.L. Khalaf, M.S. Kadhim, A.R. Khudair, Studying of COVID-19 fractional model: stability analysis, Partial Differ. Equ. Appl. Math. 7 (2023) 100470.